

Inverse bremsstrahlung contributions to Drell–Yan like processes

A.B. Arbuzov^{1,2,*}, R.R. Sadykov²

¹*Bogoliubov Laboratory of Theoretical Physics,
JINR, Dubna, 141980 Russia*

²*Dzhelepov Laboratory of Nuclear Problems,
JINR, Dubna, 141980 Russia*

Abstract

The contribution of the sub-process $\gamma q \rightarrow q'l_1\bar{l}_2$ in hadron-hadron interactions is considered. It is a part of one-loop electroweak radiative corrections for the Drell–Yan production of lepton pairs at hadron colliders. It is shown that this contribution should be taken into account aiming at the 1% accuracy of the Drell–Yan process theoretical description. Both the neutral and charged current cases are evaluated. Numerical results are presented for typical conditions of LHC experiments.

PACS: 12.15.Lk Electroweak radiative corrections; 13.40.Ks Electromagnetic corrections to strong- and weak-interaction processes; 13.85.Qk Inclusive production with identified leptons, photons, or other nonhadronic particles

1 Introduction

The Drell–Yan like processes at high energy hadron colliders provide an advanced tool for precision studies of several problems in the elementary particle phenomenology. Studies of single Z and W bosons production with the subsequent decays into leptonic pairs play a very important role in the physical programs of Tevatron [1,2] and LHC [3,4]. These processes have large cross sections and clean signatures in the detectors. That allows to reach at LHC the 1% experimental accuracy for the total cross sections of these processes as well as high precision in the measurements of differential distributions. In particular, Drell–Yan like processes are planned be used at LHC for luminosity monitoring, W mass and width measurement, detector calibration, extraction of parton density functions, new physics searches, and other purposes.

Adequately precise theoretical predictions for single Z and W production at LHC are required. For this reason we have to scrutinize several effects involved in the derivation of the theoretical accuracy: QCD and electroweak radiative corrections, uncertainties in the partonic density functions (PDF's), technical precision of Monte Carlo event generators *etc.* In this

*e-mail: arbuzov@theor.jinr.ru

paper we consider a particular contribution of the first order electroweak radiative corrections coming from the photon induced process

$$h_1 + h_2 \rightarrow X + \gamma + q \rightarrow X + q' + l_1 + \bar{l}_2, \quad (1)$$

where $h_{1,2}$ stand for the initial colliding hadrons; l_1 and \bar{l}_2 is a pair of leptons (*e.g.* μ^- and μ^+ , or ν_e and e^+); $X + q'$ denotes the remaining final state particles (typically they are hadrons). Here γ and q are treated as partons found in the initial hadrons with certain energy fractions at a given factorization scale. In this paper we use the MRST2004QED [5] parameterization of parton density functions (PDFs), which provides in particular the photon content in proton at NLO. Note that the evolution [6] of the partonic densities taking into account simultaneous QCD and QED effects leads to the unique value of the factorization scale, so that it is impossible to disentangle QED and QCD contributions. This leads also to the fact that the reduction of the factorization scale dependence can be reached now only by taking into account both QED and QCD higher order radiative corrections and that should be performed within the same factorization scheme. Nevertheless due to the smallness of the fine structure constant α in comparison with the strong coupling constant α_s , we can limit ourselves to the evaluation of only the first order electroweak corrections [7–16] together with certain higher order leading logarithmic contributions [17–19]. At the same moment QCD corrections have to be treated at least at NNLO [20–22]. Some numerical results for the inverse bremsstrahlung contribution to the charged current case (single W boson production) were already presented by S. Dittmaier and M. Krämer in the proceedings of the Les Houches workshop [23]. We performed an independent calculation and give below a comparison with the earlier results. The neutral current case is considered in addition.

This paper is organized as follows. In the next section we present the derivation of the Drell–Yan process cross sections in the scheme with massive quarks. The subtraction of the quark mass singularities is described in Sect. 3. Numerical results and their discussion are presented in Conclusions.

2 Inverse bremsstrahlung with massive quarks

Let us compute the cross section of the process (1) in the form proposed by Drell and Yan [24] as of a convolution of the parton density functions with the hard sub-process distribution. In our case the sub-processes is

$$q + \gamma \rightarrow q' + l_1 + \bar{l}_2, \quad (2)$$

where quarks q and q' are of the same type for the neutral current (NC) case and different for the charged current (CC) one. We compute the matrix element of the NC and CC sub-processes with help of the SANC system [25, 26] environment. In the actual calculation, we start within the massive quark scheme. The matching of this scheme with the PDF formalism will be performed by means of the subsequent subtraction of the quark mass singularities from the computed cross section. So, we evaluate the complete tree-level matrix elements of the sub-processes in the standard way keeping the exact dependence on the quark and lepton masses. The Feynman diagrams for the sub-processes under consideration are shown in Figs. 1 and 2.

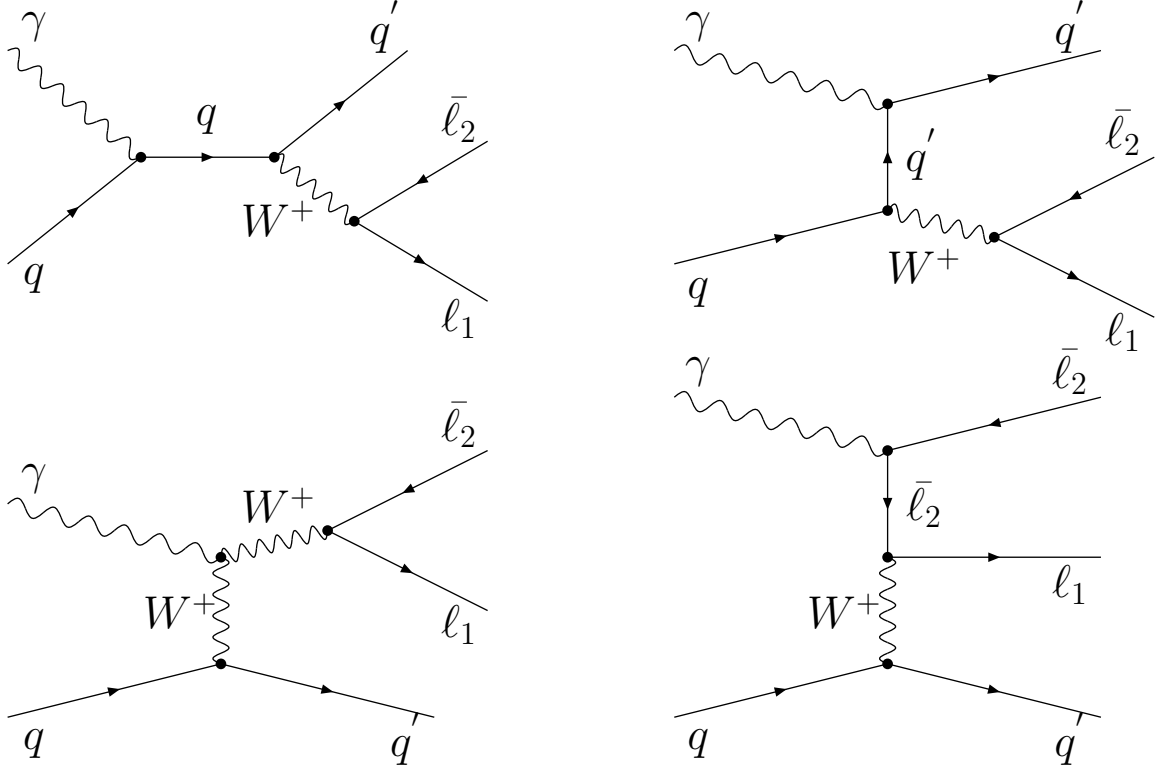


Figure 1: Feynman diagrams for inverse bremsstrahlung in the charged current Drell–Yan sub-process.

We construct the squares of the matrix elements in the usual way and obtain the partonic cross sections of the sub-processes. These quantities have to be convoluted then with the parton density functions:

$$\frac{d\sigma_{\text{inv.brem.}}^{pp \rightarrow l_1 \bar{l}_2 X}(s)}{dc_1} = \sum_{q_i} \int_0^1 \int_0^1 dx_1 dx_2 q_i(x_1, M^2) \gamma(x_2, M^2) \frac{d^2 \hat{\sigma}^{q_i \gamma \rightarrow q'_i l_1 \bar{l}_2}(\hat{s})}{d\hat{c}_1} \mathcal{J} \Theta(c_1, x_1, x_2), \quad (3)$$

where c_1 denotes the cosine of the scattering angle of the first lepton (another variable can be chosen as well). The step function $\Theta(c_1, x_1, x_2)$ defines the phase space domain corresponding to the given event selection procedure. The partonic cross section is taken in the center-of-mass reference frame of the initial partons, where the cosine of the first lepton scattering angle, \hat{c}_1 , is defined. The transformation into the observable variable c_1 involves the Jacobian:

$$\begin{aligned} \mathcal{J} &= \frac{\partial \hat{c}}{\partial c} = \frac{4x_1 x_2}{a^2}, \quad a = x_1 + x_2 - c(x_1 - x_2), \\ \hat{c} &= 1 - (1 - c) \frac{2x_1}{a}, \quad \hat{s} = s x_1 x_2, \end{aligned} \quad (4)$$

where s is the squared center-of-mass energy of the colliding hadrons. An analogous formula can be written for any other choice of a differential distribution as well as for the total cross section.

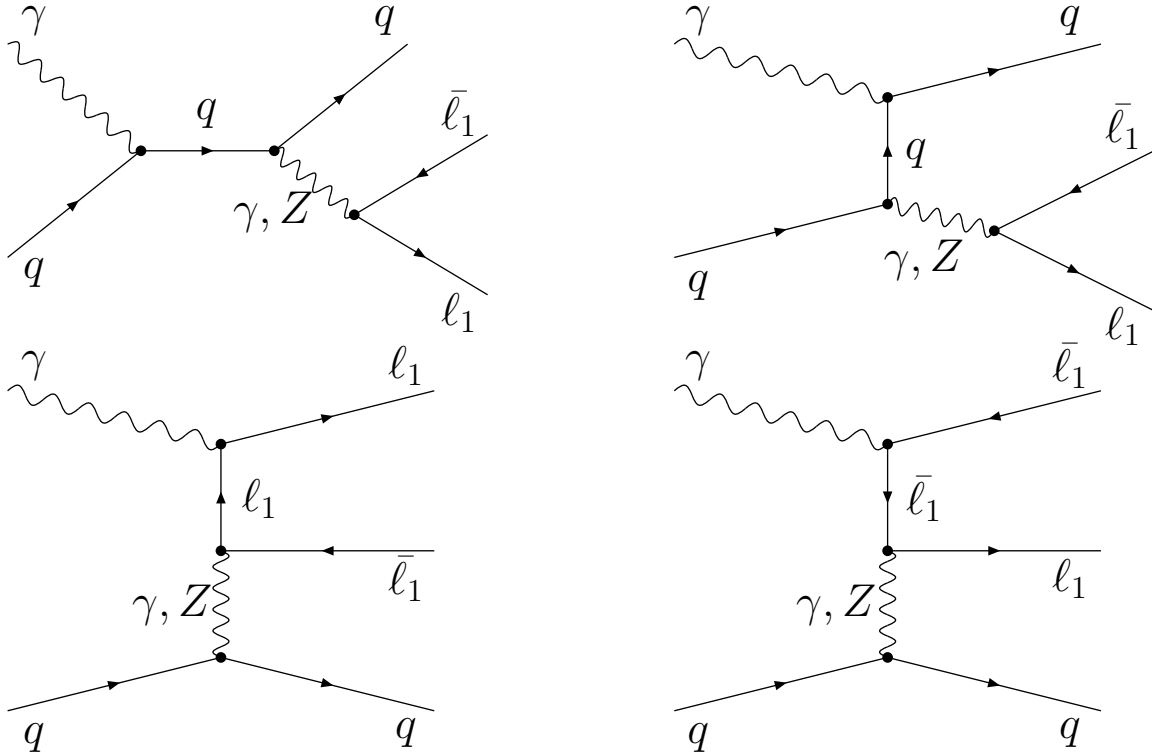


Figure 2: Feynman diagrams for inverse bremsstrahlung in the neutral current Drell–Yan sub-process.

In Eq. (3) we presented the contribution, when the photon is found in the first of the colliding hadrons and the quark is taken from the other one. Of course, there is also the contribution when we choose the particles in the other way round, and it is taken into account in our numerical simulations.

3 Subtraction of the quark mass singularities

Since the calculation of the partonic cross sections was performed keeping finite masses of the quarks, the result (3) depends on the values of the masses. For the high energies this dependence arises in the form of large logarithms of the type $\ln(M^2/m_q^2)$ that give a considerable numerical effect, while the other mass-dependent contributions suppressed by the factor $m_q^2/M^2 \ll 1$ can be omitted (here M is a typical energy scale of the partonic sub-process). The large logarithms represent quark mass singularities. They can be treated with help of the QED renormalization group approach. But the point is that they have been already taken into account in the evolution of partonic density functions. In the MRST2004QED distributions [5] that have been done explicitly. But even in any other PDF on the market the QED evolution is implicitly taken into account since it has not been subtracted from the experimental data before the PDF fitting procedure. In fact, QED corrections to the quark line in deep inelastic scattering are usually omitted in the data analysis, see Refs. [27, 28].

The quark mass singularity of the first type arises from the right Feynman diagrams in the

upper line of Fig. 1 and of Fig. 2 for CC and NC cases, respectively. The singularity originates from the kinematical domain when the virtual quark propagator is close to the mass shell. For this situation there is a convolution of distributions of the two sub-processes: a conversion of the photon into a pair of quarks and a Drell–Yan partonic process $q' + q \rightarrow l_1 \bar{l}_2$. In the $\overline{\text{MS}}$ scheme the corresponding contribution reads

$$\begin{aligned} \delta_1(c_1) &= \sum_{q_i} \int_0^1 \int_0^1 dx_1 dx_2 \gamma(x_1, M^2) q_i(x_2, M^2) \int_0^1 dx_3 D_{q'\gamma}(x_3, M, m_{q'}) \\ &\times \frac{d^2 \tilde{\sigma}^{q_i q'_i \rightarrow l_1 \bar{l}_2}(\tilde{s})}{d\tilde{c}_1} \tilde{\mathcal{J}} \Theta(c_1, x_1 x_3, x_2), \end{aligned} \quad (5)$$

where \tilde{c}_1 , $\tilde{\mathcal{J}}$ and \tilde{s} are calculated according to Eq. (4) with the interchange $x_1 \rightarrow x_1 x_3$. For the NC case in the above equation we have $q' = q$. The structure function $D_{q'\gamma}(x_3, M, m_{q'})$ describes the probability to find quark q' with energy fraction x_3 in the photon. For the $\overline{\text{MS}}$ scheme at NLO this function reads

$$D_{q'\gamma}^{\overline{\text{MS}}}(x_3, M, m_{q'}) = \frac{\alpha}{2\pi} Q_{q'}^2 \ln \frac{M^2}{m_{q'}^2} [x_3^2 + (1 - x_3)^2], \quad (6)$$

where M is the factorization scale, and $Q_{q'}$ is the quark charge.

In the neutral current case there is one additional source of the quark mass singularities. It arises from the two lower Feynman amplitudes in Fig. 2, when the virtual photon propagator is near the mass shell. In this case we have the convolution of the distributions of the following processes: $2\gamma \rightarrow l_1 \bar{l}_1$ and $q \rightarrow \gamma q$. The corresponding contribution is

$$\begin{aligned} \delta_2(c_1) &= \sum_{q_i} \int_0^1 \int_0^1 dx_1 dx_2 q_i(x_1, M^2) \gamma(x_2, M^2) \int_0^1 dx_3 D_{\gamma q}(x_3, M, m_q) \\ &\times \frac{d^2 \tilde{\sigma}^{\gamma\gamma \rightarrow l_1 \bar{l}_1}(\tilde{s})}{d\tilde{c}_1} \tilde{\mathcal{J}} \Theta(c_1, x_1 x_3, x_2). \end{aligned} \quad (7)$$

The relevant structure function describes the probability to find a photon with a certain energy fraction in the quark:

$$D_{\gamma q}^{\overline{\text{MS}}}(x_3, M, m_q) = \frac{\alpha}{2\pi} Q_{q'}^2 \frac{1 + (1 - x_3)^2}{x_3} \left\{ \ln \frac{M^2}{m_q^2} - 2 \ln x_3 - 1 \right\}, \quad (8)$$

According to the renormalization formalism we have now to subtract the contributions (5) and (7) from the computed cross section (3). In a realistic situation we have to perform this procedure numerically in order to keep the possibility to impose experimental cuts. On the other hand, it can be shown analytically that the terms with the logarithms of the quark masses do cancel out during the subtraction procedure.

4 Numerical Results and Conclusions

For the numerical evaluations we used the same conditions and the input parameters as in Ref. [23]:

$$\begin{aligned}
 G_F &= 1.16637 \times 10^{-5} \text{ GeV}^{-2}, \\
 \alpha(0) &= 1/137.03599911, & \alpha_s &= 0.1187, \\
 M_W &= 80.425 \text{ GeV}, & \Gamma_W &= 2.124 \text{ GeV}, \\
 M_Z &= 91.1867 \text{ GeV}, & \Gamma_Z &= 2.4952 \text{ GeV}, \\
 M_H &= 150 \text{ GeV}, & m_t &= 174.17 \text{ GeV}, \\
 m_u &= m_d = 66 \text{ MeV}, & m_c &= 1.55 \text{ GeV}, \\
 m_s &= 150 \text{ MeV}, & m_b &= 4.5 \text{ GeV}, \\
 |V_{ud}| &= |V_{cs}| = 0.975, & |V_{us}| &= |V_{cd}| = 0.222.
 \end{aligned}$$

The MRST204QED set [5] of PDF's and the G_F EW scheme were used. The cut on the charged lepton rapidity and transverse momentum are $|\eta_\ell| < 1.2$ and $P_{T,\ell} > 25 \text{ GeV}$. The cut on the missing transverse momentum for the CC case is imposed as well: $P_{T,\text{missing}} > 25 \text{ GeV}$.

At the partonic level for the CC and NC processes ($\gamma + q \rightarrow q' + l_1 + \bar{l}_2$) we performed a comparison with the corresponding distributions obtained with help of the CompHEP system [29] and found a good agreement.

$P_{T,\mu}/\text{GeV}$	25 – ∞	50 – ∞	100 – ∞	200 – ∞	500 – ∞	1000 – ∞
σ_0/pb						
DK	2112.2(1)	13.152(2)	0.9452(1)	0.11511(2)	0.0054816(3)	0.00026212(1)
SANC	2112.2(1)	13.151(1)	0.9451(1)	0.11511(1)	0.0054813(1)	0.00026211(1)
$\delta_{\gamma q}/\%$						
DK	0.071(1)	5.24(1)	13.10(1)	16.44(2)	14.30(1)	11.89(1)
SANC	0.074(1)	5.24(1)	13.09(1)	16.43(1)	14.30(1)	11.90(1)

Table 1: Cross sections σ_0 and $\sigma_{\gamma q}$ of the processes $p[q]p[q'] \rightarrow \nu_\mu \mu^+ X$ and $p[\gamma]p[q] \rightarrow \nu_\mu \mu^+ X$, respectively and corresponding corrections $\delta_{\gamma q} = \sigma_{\gamma q}/\sigma_0$, obtained by DK and SANC groups for different $P_{T,\mu}$ ranges at LHC.

In Table 1 we present the results of comparison for the inverse bremsstrahlung contribution to the CC Drell–Yan process with different cuts on the charged lepton transverse momentum (see the details in Ref. [23]). Our results are marked as “SANC”, they are compared with the numbers (“DK”) presented by the S. Dittmaier and M. Krämer in Ref. [23]. The small deviations in the results for the values of the corrections are certainly beyond the 1% precision level. They are due to some differences in the schemes of calculations and are induced by higher order effects in α .

Table 2 shows the results of comparison for the inverse bremsstrahlung contribution to CC Drell–Yan process with different cuts on transverse mass of muon-neutrino pair. The corresponding numbers for $\delta_{\gamma q}$ are below percent level.

Table 3 gives the results for the inverse bremsstrahlung contribution to the neutral current Drell–Yan process with production of two muons. Different values of the cut on the invariant mass of the muon pair are considered. For the Born cross section we show also the numbers of HORACE [17, 19], which are in fair agreement with the SANC results.

$M_{T,\nu\mu^+}/\text{GeV}$	50 – ∞	100 – ∞	200 – ∞	500 – ∞	1000 – ∞	2000 – ∞
σ_0/pb						
DK	2112.2(1)	13.152(2)	0.9452(1)	0.057730(5)	0.0054816(3)	0.00026212(1)
SANC	2112.2(1)	13.151(1)	0.9451(1)	0.057730(5)	0.0054813(1)	0.00026211(1)
$\delta_{\gamma q}/\%$						
DK	0.0567(3)	0.1347(1)	0.2546(1)	0.3333(1)	0.3267(1)	0.3126(1)
SANC	0.0532(1)	0.1350(1)	0.2537(1)	0.3314(1)	0.3245(1)	0.3094(1)

Table 2: Cross sections σ_0 and $\sigma_{\gamma q}$ of the processes $p[q]p[q'] \rightarrow \nu\mu\mu^+X$ and $p[\gamma]p[q] \rightarrow \nu\mu\mu^+X$, respectively and corresponding corrections $\delta_{\gamma q} = \sigma_{\gamma q}/\sigma_0$, obtained by DK and SANC groups for different $M_{T,\nu\mu^+}$ ranges at LHC.

$M_{\mu^+\mu^-}/\text{GeV}$	50 – ∞	100 – ∞	200 – ∞	500 – ∞	1000 – ∞	2000 – ∞
σ_0/pb						
HORACE	254.64(1)	10.571(1)	0.45303(3)	0.026996(2)	0.0027130(2)	0.00015525(1)
SANC	254.65(2)	10.571(1)	0.45308(3)	0.026996(2)	0.0027131(2)	0.00015525(1)
$\delta_{\gamma q}/\%$						
SANC	0.047(1)	0.449(1)	0.013(1)	0.496(1)	0.619(1)	0.563(1)

Table 3: Cross sections σ_0 and $\sigma_{\gamma q}$ of the processes $p[q]p[q'] \rightarrow \mu^+\mu^-X$ and $p[\gamma]p[q] \rightarrow \mu^+\mu^-X$, respectively and corresponding corrections $\delta_{\gamma q} = \sigma_{\gamma q}/\sigma_0$, for different $M_{\mu^+\mu^-}$ ranges at LHC.

In Fig. 3 we plotted the distributions of the Born-level cross section and of the relative radiative correction versus the transverse mass of the muon and neutrino pair $M_T(\mu^+\nu_\mu)$ in the CC Drell-Yan process,

$$M_T(\mu^+\nu_\mu) = \sqrt{2P_{T,\mu}P_{T,\nu}(1 - \cos\phi_{\mu\nu})}, \quad (9)$$

where $\phi_{\mu\nu}$ is the angle between the muon momentum and the missing one in the transverse plane. In Fig. 4 the analogous distributions in the muon transverse momentum $P_{T,\mu}$ are given.

Fig. 5 shows the Born differential cross section of the neutral current Drell-Yan process **(a)** and the relative correction $\delta_{\gamma q}$ **(b)** as a function of invariant mass $M_{\mu^+\mu^-}$ of the muon pair. Fig. 6 gives us results for the Born differential cross section of the neutral current Drell-Yan process **(a)** and the relative correction $\delta_{\gamma q}$ **(b)** as a function of μ^+ transverse momentum $P_{T,\mu}$. The distributions around the W and Z resonances are plotted. The drop-offs in the first bins of the correction distributions in NC have no any physical sense. They arise because the factorization procedure with the longitudinal partonic density functions doesn't allow to apply the experimental cuts unambiguously. The drop-offs can be shifted by choosing a different cut value. We checked that the rest of the distributions doesn't suffer from this problem.

In this way we presented the photon-induced contribution to the first order electroweak radiative corrections to Drell-Yan processes. For the case of charged current scattering our results are in a good agreement with earlier calculations of the other group. The neutral current case was considered in an analogous manner. This inverse bremsstrahlung contribution should be taken into account together with all other relevant effects to reach the accuracy of the Drell-Yan process theoretical description adequate to the precision of the forthcoming LHC experiments. The typical size of the contribution is below one percent, but for the

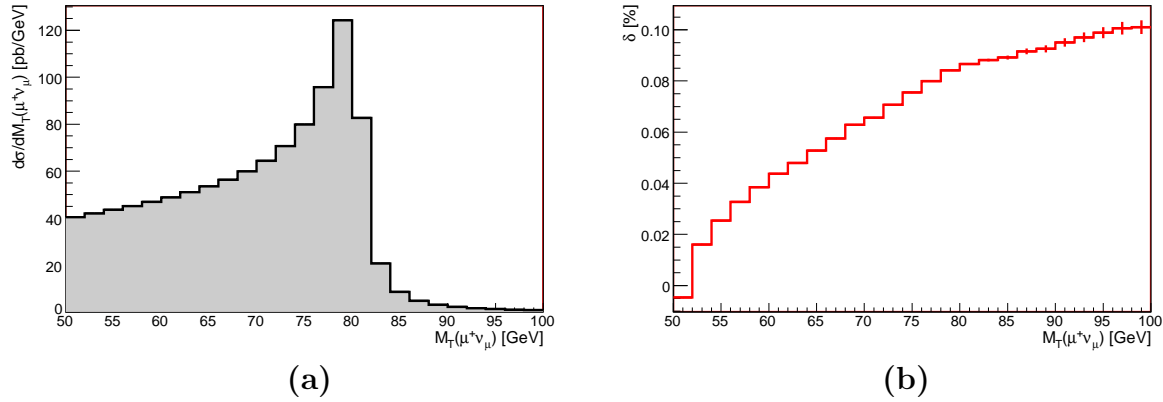


Figure 3: The Born-level CC Drell–Yan cross section and the relative contribution of the inverse bremsstrahlung versus the transverse mass of the muon-neutrino pair.

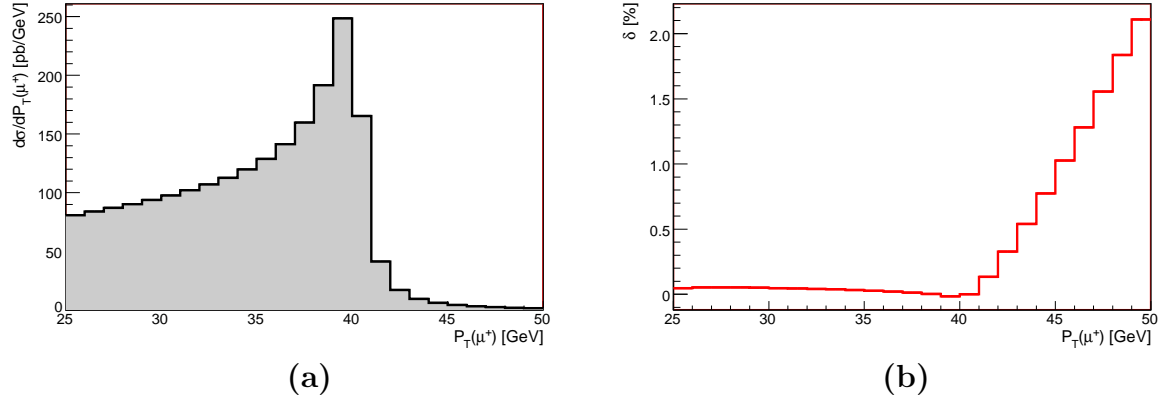


Figure 4: The Born-level CC Drell–Yan cross section and the relative contribution of the inverse bremsstrahlung versus the μ^+ transverse momentum.

case of transverse momentum distribution in CC scattering, the effect can reach up to 16% depending on the cut value. We are going to implement the results of our calculations into a general Monte Carlo event generator for Drell–Yan processes, which is under development in the SANC group.

Acknowledgements

We are grateful to D. Bardin, S. Bondarenko, P. Christova, L. Kalinovskaya for fruitful discussions and critical reading of the manuscript. This work was supported by the RFBR grant 07-02-00932. One of us (A.A.) thanks also the grant of the President RF (Scientific Schools 5332.2006) and the INTAS grant 03-51-4007.

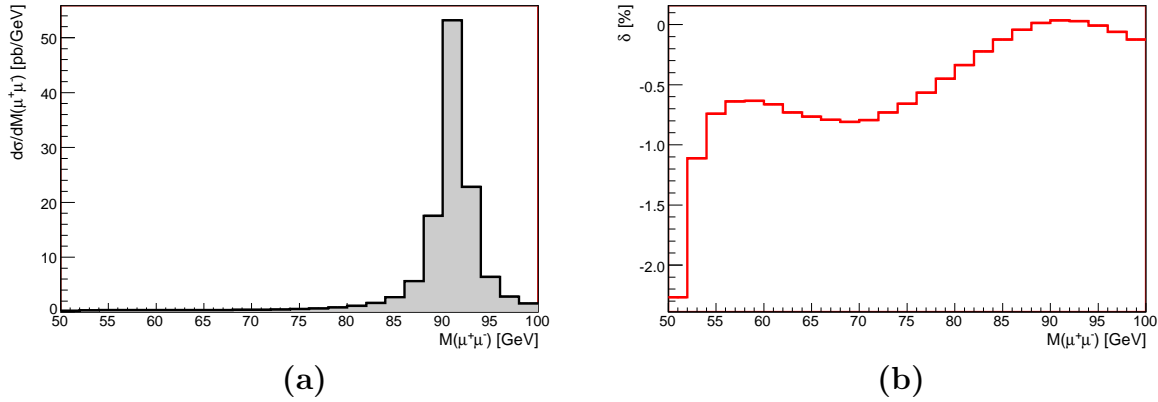


Figure 5: The Born-level NC Drell–Yan cross section and the relative contribution of the inverse bremsstrahlung versus the invariant mass of the muon pair.

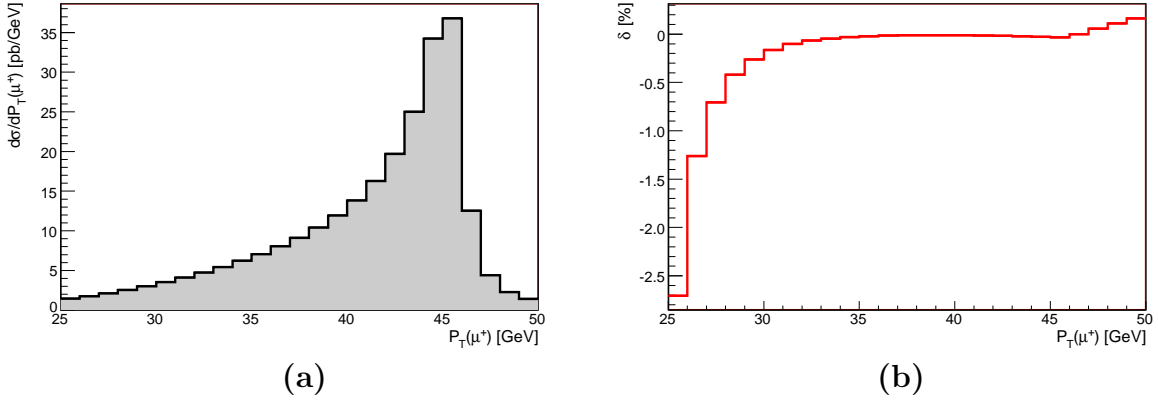


Figure 6: The Born-level NC Drell–Yan cross section and the relative contribution of the inverse bremsstrahlung versus the μ^+ transverse momentum.

References

- [1] V.M. Abazov *et al.* [CDF Collaboration], Phys. Rev. D **70**, 092008 (2004).
- [2] S. Abachi *et al.* [D0 Collaboration], Phys. Rev. Lett. **77** (1996) 3309.
- [3] G. Altarelli and M.L. Mangano, *Standard model physics (and more) at the LHC*, Workshop Proceedings, CERN Report 2000-04, p.117.
- [4] N.V. Krasnikov and V.A. Matveev, Phys. Part. Nucl. **28** (1997) 441; and references therein.
- [5] A.D. Martin, R.G. Roberts, W.J. Stirling and R.S. Thorne, Eur. Phys. J. C **39** (2005) 155.

- [6] M. Roth and S. Weinzierl, Phys. Lett. B **590** (2004) 190.
- [7] V.A. Mosolov and N.M. Shumeiko, Nucl. Phys. B **186** (1981) 397.
- [8] A.V. Soroko and N.M. Shumeiko, Sov. J. Nucl. Phys. **52** (1990) 329.
- [9] D. Wackeroth and W. Hollik, Phys. Rev. D **55** (1997) 6788.
- [10] U. Baur, S. Keller and D. Wackeroth, Phys. Rev. D **59** (1999) 013002.
- [11] S. Dittmaier and M. Krämer, Phys. Rev. D **65** (2002) 073007.
- [12] U. Baur, O. Brein, W. Hollik, C. Schappacher and D. Wackeroth, Phys. Rev. D **65** (2002) 033007.
- [13] U. Baur and D. Wackeroth, Phys. Rev. D **70** (2004) 073015.
- [14] C. M. Carloni Calame, G. Montagna, O. Nicrosini and A. Vicini, JHEP **0612** (2006) 016.
- [15] V.A. Zykunov, Phys. Atom. Nucl. **69** (2006) 1522.
- [16] A. Arbuzov, D. Bardin, S. Bondarenko, P. Christova, L. Kalinovskaya, G. Nanava and R. Sadykov, Eur. Phys. J. C **46** (2006) 407.
- [17] C.M. Carloni Calame, G. Montagna, O. Nicrosini and M. Treccani, Phys. Rev. D **69** (2004) 037301.
- [18] C.M. Carloni Calame, G. Montagna, O. Nicrosini and M. Treccani, Eur. Phys. J. C **33**, S665 (2004).
- [19] C. M. Carloni Calame, G. Montagna, O. Nicrosini and M. Treccani, JHEP **0505** (2005) 019.
- [20] C. Anastasiou, L. J. Dixon, K. Melnikov and F. Petriello, Phys. Rev. Lett. **91** (2003) 182002.
- [21] C. Anastasiou, L. J. Dixon, K. Melnikov and F. Petriello, Phys. Rev. D **69** (2004) 094008.
- [22] K. Melnikov and F. Petriello, Phys. Rev. D **74** (2006) 114017.
- [23] C. Buttar *et al.*, *Les Houches physics at TeV colliders 2005, standard model, QCD, EW, and Higgs working group: Summary report*, hep-ph/0604120.
- [24] S.D. Drell and T.M. Yan, “Massive Lepton Pair Production In Hadron - Hadron Collisions At Phys. Rev. Lett. **25** (1970) 316, *Erratum ibid.* **25** (1970) 902.
- [25] A. Andonov, A. Arbuzov, D. Bardin, S. Bondarenko, P. Christova, L. Kalinovskaya, G. Nanava and W. von Schlippe, *SANCScope - v.1.00*, Comput. Phys. Commun. **174** (2006) 481; *Erratum ibid.* doi:10.1016/j.cpc.2007.06.010; and references therein.
- [26] D. Bardin, S. Bondarenko, L. Kalinovskaya, G. Nanava, L. Rummyantsev and W. von Schlippe, *SANCSnews: Sector f f b b*, hep-ph/0506120, to appear in Comp. Phys. Commun.

- [27] A. A. Akhundov, D. Y. Bardin, L. Kalinovskaya and T. Riemann, Fortsch. Phys. **44** (1996) 373.
- [28] A. Arbuzov, D. Y. Bardin, J. Bluemlein, L. Kalinovskaya and T. Riemann, Comput. Phys. Commun. **94** (1996) 128.
- [29] E. Boos *et al.* [CompHEP Collaboration], Nucl. Instrum. Meth. A **534** (2004) 250.